

*Short Communication*

## **Study the Corrosion Inhibition of Carbon Steel in 1 M HCl Using Extracts of Date Palm Waste**

*Ghadah M. Al-Senani and Mashael Alshabanat*

Department of Chemistry, College of Science, Princess Nourah bint Abdulrahman University, Riyadh, Saudi Arabia

E-mail: [gmalsnany@pnu.edu.sa](mailto:gmalsnany@pnu.edu.sa), [ghada-moh@hotmail.com](mailto:ghada-moh@hotmail.com)

*Received: 25 November 2017 / Accepted: 17 January 2018 / Published: 6 March 2018*

---

In this study, extracts of both treated and untreated date palm tree waste were used as inhibitors of carbon steel corrosion in 1 M HCl. The date palm wastes used were the fiber and leaflets of the plant, and the treatment process involved gum arabic solution. The electrochemical measurements showed that the extracts were efficient inhibitors. The treated wastes were more efficient inhibitors than untreated waste, and the leaflets were better inhibitors than the fibers. The effect of temperature on inhibition efficiency, thermodynamic parameters, and adsorption isotherms for the treated inhibitors were studied. It was found that the adsorption was endothermic, occurred spontaneously, and that the adsorption data fit Langmuir isotherm model.

---

**Keywords:** Carbon steel, Hydrochloric acid, Corrosion inhibition, Date palm, Adsorption

### **1. INTRODUCTION**

Carbon steel is used worldwide as pipelines for transferring liquids and gases, which leads to rust formation. Although rust can be removed by treatment with hydrochloric acid and sulfuric acid, this leads to severe corrosion. Therefore, the protection of metals from corrosion is very important in industries, especially in acidic mediums, for which the use of inhibitors is one of the methods.

Generally, organic compounds are good inhibitors; however, they are not environment-friendly because of their high toxicity. Therefore, the need to use natural materials as alternative inhibitors is acceptable. Corrosion inhibition using various plant extracts has been reported; for example, *Cucumis sativus* [1], *Petroselinum crispum*, *Eruca sativa*, *Anethum graveolens* [2], *Coriandrum sativum* leaves [3], Banana peel [4], *Gnetum africana* leaves [5], *Eriobotrya japonica* thunb. leaf extract [6], *Sesbania sesban* extract [7] have been investigated.

Date palm is an important cultivated plant in many countries, where it grows in dry and semi-arid regions. It is considered one of the main agricultural crops in Saudi Arabia. Saudi has more than 23 million palm trees that produce about one million tons of dates per year, and the wastes include palm veins, leaves, stems, leaflet, and fibers [8]. Usually, the waste residues are burned on farms or buried in landfills, causing environmental pollution. Therefore, reusing date palm waste seems an optimal solution at environmental and economical levels. Thus, using these materials to produce cheap, sustainable, and ecofriendly inhibitors of carbon steel corrosion is quite interesting. The effectiveness of fibers and leaflets as corrosion inhibitors using electrochemical measurements, thermodynamics, and adsorption studies is yet to be reported; this is the aim of the current study.

## 2. EXPERIMENTAL

### 2.1. Preparation of inhibitor

Fibers and leaflet parts of date palm (Figure 1) [9] were collected from a local farm, cut, grinded, and sieved to obtain particle size  $\leq 600 \mu\text{m}$ . The powder was divided into two parts: one was not pretreated and the other was treated. A natural treatment process was performed by washing the desired amount of sieved powder with distilled water followed by washing with gum arabic (GA) solution in an electric mixer. The mixture was subsequently sonicated, passed through a mesh, and dried for a few days in sunlight. The specimens were labeled **PF**, **PL**, **PF-T**, and **PL-T**, for untreated fiber, untreated leaflet, treated fiber, and treated leaflet, respectively.

Then, 2 g from the dried powder was mixed with 200 mL of 1 M HCl and refluxed at 50 °C for 2 h. The extracts were cooled and filtered through Whatman filter paper. The filtrate (25-30%, wt. %) was then kept as the stock solution, from which test solutions of concentrations ranging from 1 to 20% (v/v) were prepared by dilution with 1 M HCl solution.

### 2.2. Characterization of the inhibitors

Fourier-transform infrared (FT-IR) spectra were recorded from 400 to 4000  $\text{cm}^{-1}$  using a Perkin–Elmer spectrophotometer to analyze the structure, for which the samples were prepared in the form of KBr pellets containing the powdered samples. A scanning electron microscope (SEM, Quanta 250) was used to study the surface morphology.



**Figure 1.** Palm leaflet, Palm fiber

### 2.3 Specimen Preparation

Carbon steel specimens (C 0.1%, Mn 1.23%, Si 0.265%, S 0.004%, P 0.011%, Cr 0.008%, Cu 0.024%, Si 0.0016%, Ni 0.0214%, Ti 0.017%, Al 0.035%, Nb 0.036%, Ca 0.002%, CEV 0.319%, and Fe balance). It was cut from a carbon steel rod with a cross-sectional area of 1 cm<sup>2</sup> and was embedded in a Teflon holder. The specimens were polished with 800 and 1200 grit grinding papers, and cleaned by distilled water and acetone.

### 2.4 Electrochemical measurements

Electrochemical measurements were performed using the 1783 tool model. The electrochemical cell contains a three-electrode configuration with a conventional graphite electrode as the counter electrode and a saturated calomel electrode (SCE) coupled with a Luggin-Haber capillary as the reference electrode.

The working electrode was immersed in 1 M HCl solutions with and without 1, 5, 10, 15, 20% of **PF**, **PL**, **PF-T**, and **PL-T** extracts at 25 °C and 60 °C; the open circuit potential was measured after 10 min to achieve steady state.

Potentiodynamic polarization studies were performed with a scan rate of 0.2 mVs<sup>-1</sup> in the potential range of ±250 mV proportional to the potential of corrosion. The inhibition efficiency (E<sub>inh</sub>%) was calculated using Eq. 1:

$$E_{inh} \% = \frac{I_{corr} - I_{corr(inh)}}{I_{corr}} \times 100 \quad (1)$$

where I<sub>corr</sub> and I<sub>corr(inh)</sub> are referred to as the corrosion current densities without and with the inhibitor, respectively.

## 3. RESULTS AND DISSCUSION

### 3.1. Characterization of the inhibitors

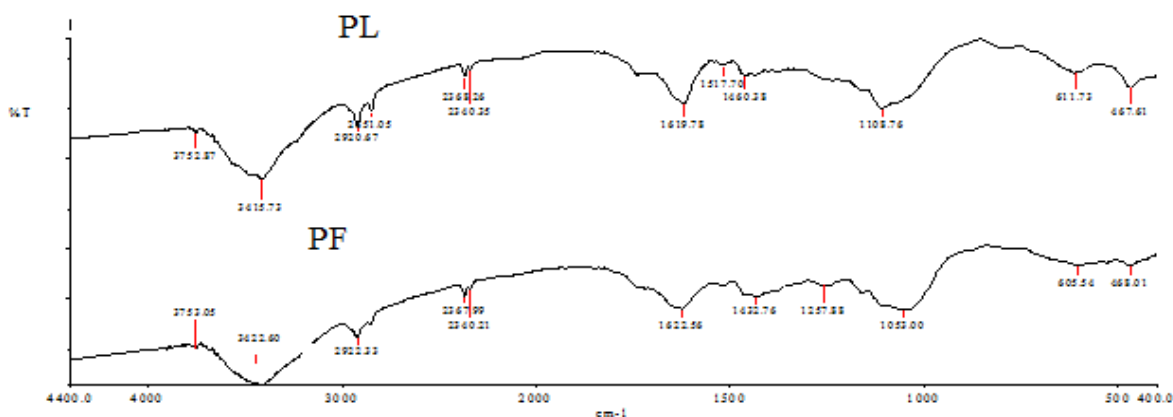
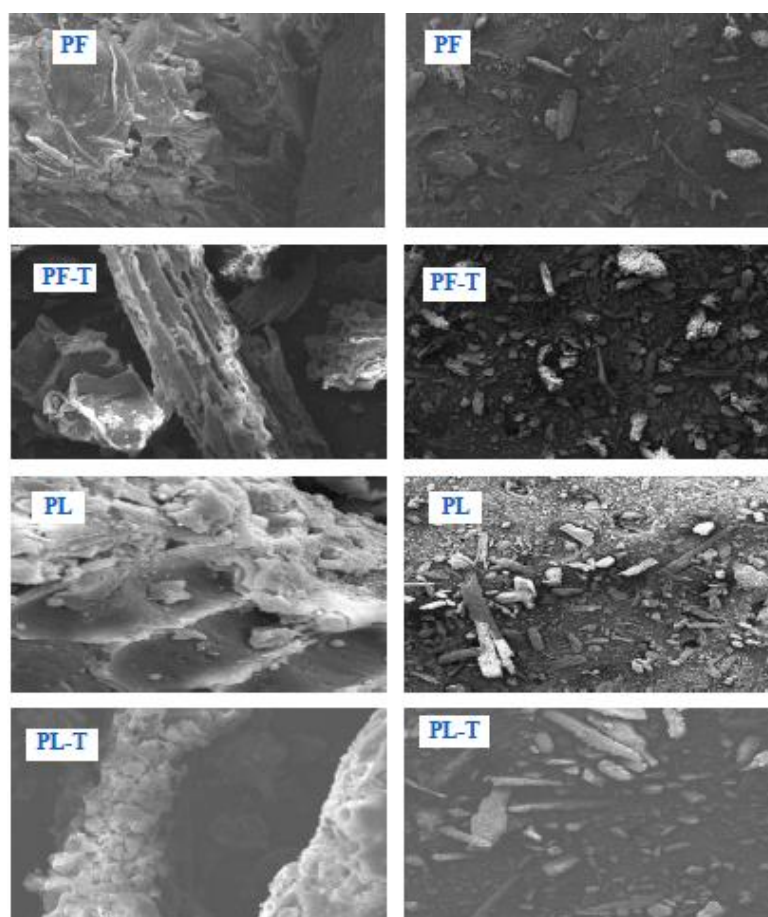


Figure 2. FT-IR of untreated fiber and leaflet

Figure 2 shows the IR absorption bands of fibers and leaflets. The peaks indicate the presence of functional groups containing S, P, O, and N, atoms attached to aromatic rings, which are usually distinguished of corrosion inhibitors (Table 1).

**Table 1.** FT-IR of untreated fiber and leaflet

Peaks from FT-IR spectra	Possible functional groups
617.89	-C=C stretch
1068.10	P-O-C stretch
1247.46	O-SO <sub>2</sub> -O
1411.10	X-SO <sub>2</sub> -X
1614.22	C=N stretch
2927.20	C-H (aromatic)
3339.39	N-H stretch



**Figure 3.** SEM images of treated and untreated fiber and leaflet

Figure 3 shows the SEM images of treated and untreated specimens of the inhibitors. Irregular shapes and different sizes of the powder were noticed irrespective of whether the specimens were treated or untreated. Comparison between the treated and untreated specimens showed some holes and deep cracks on the surfaces after treatment, which seem to be active sites and are suited for bending.

### 3.2. Potentiodynamic polarization

#### 3.2.1. At room temperature:

Potentiodynamic polarization measurement were performed to determine the kinetics of the anodic and cathodic reactions. Figure 4 shows the typical polarization curves of carbon steel in 1 M HCl solutions with **PF**, **PF-T**, **PL**, and **PL-T** concentrations of (0, 1, 5, 10, 15, and 20)%.

The addition of treated and untreated inhibitors makes the oxidation potential more negative. As shown, the corrosion voltage of carbon steel is deviated to the negative direction. A 2% decrease is observed in the value of the corrosion current in the presence of **PF-T** compared to that in the presence of **PF**.

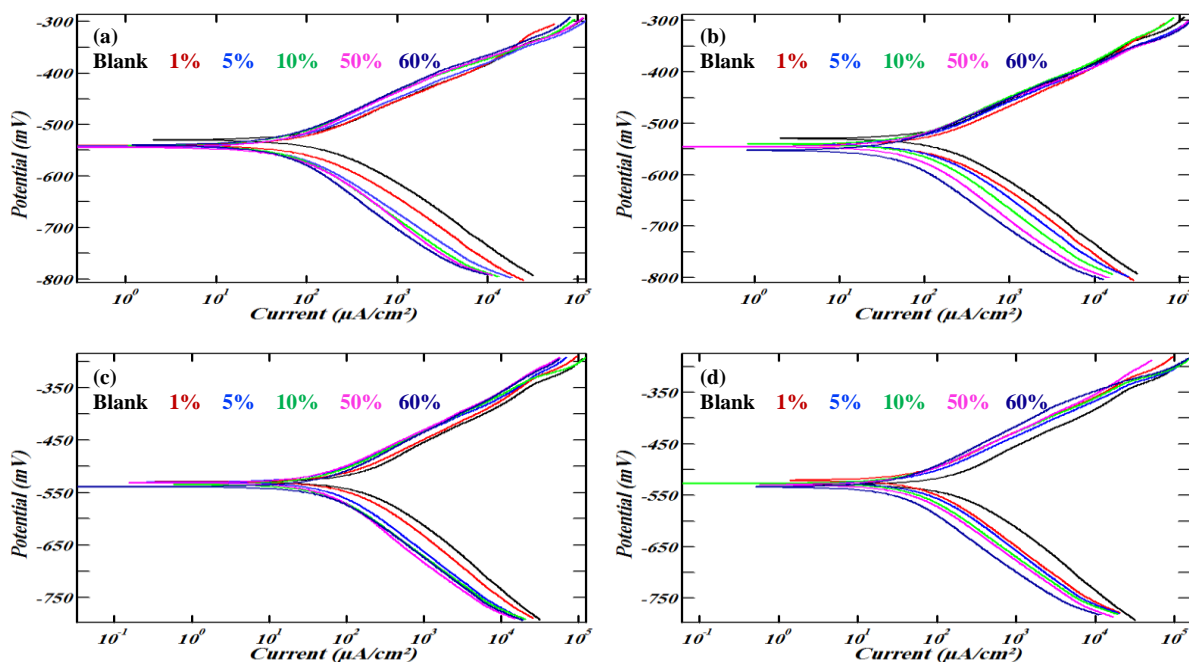
Both the corrosion rate and the corrosion current were significantly reduced in the presence of **PL-T** compared to that in the presence of **PL**. Furthermore, the electrode reactions were affected by the addition of both types of inhibitors, the treated and untreated (Figure 4). The inhibitors also affected the cathodic reaction more than the anodic reaction, suggesting that the reaction is controlled by hydrogen evolution.

Table 2 summarizes the electrochemical parameters obtained from the test for all the inhibitors used. A significant improvement was observed in the corrosion resistance of carbon steel in 1 M HCl: corrosion rates were reduced upon increasing the concentration of the inhibitor extracts. Additionally,  $\beta_a$  and  $\beta_c$  values, obtained from Tafel slopes, suggest that the inhibitors act as mixed types of inhibitor affected by both hydrogen evolution and carbon steel dissolution.

Moreover, the inhibitors recorded high efficiencies, 85–89% for the treated specimens and 83–88% for the untreated ones. Both **PL** and **PL-T** were found to be have higher efficiency than **PF** and **PF-T**, respectively, by ~4%.

This means that the inhibition process involves blocking the available metal spaces and inhibiting carbon steel oxidation, with lower hydrogen evolution. The adsorption of the inhibitor particles on the surface of carbon steel forms a barrier that impedes the arrival of hydrogen ions to the surface of the steel. This reduces the  $H^+$  concentration at the cathode sites, thus reducing corrosion. [10-11].

The efficiencies of different palm extracts were compared with those of some plant extracts previously studied by potentiodynamic polarization method, as shown in Table 3 and Figure 5. Palm extracts showed high efficiency (85-89%) as an inhibitor of carbon steel corrosion in 1 M HCl at 20% (V/V) and 25 °C [1-3, 7, 12, 13].



**Figure 4.** Polarization curves for carbon Steel in 1 M HCl with and without 1, 5, 10, 15% and 20% of (a) PF, (b) PF-T, (c) PL and (d) PL-T extracts at 25°C.

**Table 2.** Electrochemical parameters for Carbon Steel in 1 M HCl with and without 1, 5, 10, 15% and 20% of PF, PF-T, PL and PL-T extracts at 25°C.

Inhibitor Extract	Concentration (v/v)%	$-E_{corr}$ (mV)	$\beta_a$ (mV)	$\beta_c$ (mV)	$I_{corr}$ (mA cm <sup>-2</sup> )	C.R (mm/year)	$E_{inh}$ %
	Blank	528	92	121	4.54	52.25	0
PF	1	537	89	120	1.17	13.43	74
	5	539	75	113	1	11.46	78
	10	540	74	109	0.89	10.27	80
	15	540	74	106	0.84	9.72	81
	20	541	73	104	0.74	8.58	84
PF-T	1	539	85	117	1.09	12.49	76
	5	541	81	113	0.94	10.92	79
	10	542	80	108	0.86	9.80	81
	15	545	71	106	0.73	8.44	84
	20	553	71	102	0.68	7.76	85
PL	1	529	85	115	0.95	10.99	79
	5	530	77	108	0.80	9.23	82
	10	531	71	103	0.68	7.90	85
	15	532	71	100	0.59	6.71	87
	20	539	71	93	0.54	6.26	88
PL-T	1	322	78	109	0.89	10.23	80
	5	523	71	107	0.76	8.73	83
	10	528	70	98	0.67	7.63	85
	15	529	68	93	0.57	6.53	88
	20	534	68	92	0.51	5.86	89

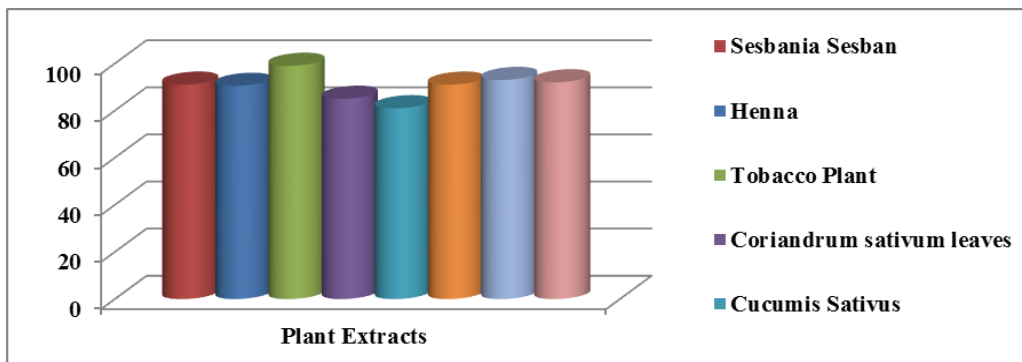


**Figure 5.** Comparison of the inhibition efficiency of Carbon Steel in 1 M HCl with inhibitors at 25°C.

**Table 3.** Plant extracts investigated as corrosion inhibitors of Carbon Steel in 1 M HCl at 25°C. by other authors.

Plant Extracts	Concentration	$E_{inh}\%$
Sesbania Sesban	2 (g/L)	91
henna	2 (g/L)	90.5
Tobacco Plant	0.3 (g/L)	99
Coriandrum sativum leaves	60% (v/v)	85
Cucumis Sativus	50% (v/v)	81
Petroselinum Crispum (Parsley)	60% (v/v)	91
Eruca Sativa (Arugula)	60% (v/v)	93
Anethum Graveolens (Dill)	60% (v/v)	92

3.2.2. At 60°C:

Potentiodynamic polarization studies of carbon steel in 1 M HCl solution were performed at 60 °C and **PF-T** and **PL-T** extracts of different concentrations. Table 4 shows the electrochemical parameters obtained for all the inhibitors used. Figure 6 and Table 3 show that the  $E_{corr}$  values shift to more negative values at different concentrations of the treated inhibitors. In addition, current densities of anodic and cathodic reactions were decreased upon increasing the concentrations of treated inhibitors. This can be explained by the adsorption of inhibitor molecules on the surface of carbon steel, forming a protective layer on the surface.

Moreover, the inhibitor's efficiency decreased at **PF-T** concentrations of 1 and 5% and **PL-T** concentration of 1%, due to the weakness of the protective layer on the surface of carbon steel and its ease of dissolution. At higher concentrations (10–20%) of both inhibitors **PF-T** and **PL-T**, inhibitor efficiency increased with increasing concentration. This is explained by the strong adsorption of organic compounds containing O, S, P, and N atoms attached to aromatic rings in their molecules, through which they can adsorb on the carbon steel surface [14, 15]. Generally, the adsorption of an inhibitor depends on its chemical structure, its molecular size, the nature and charge on the metal surface, and charge distribution over the entire inhibitor molecule. The adsorption can occur via the replacement of solvent molecules from the metal surface by ions and molecules accumulated near the

carbon steel surface. Since the inhibitor molecules can be adsorbed on the surface of carbon steel through chemisorption, involving the displacement of water molecules from the carbon steel surface and sharing of electrons between the heteroatoms and iron. The inhibitor molecules can also adsorb on the carbon steel surface by donor-acceptor interactions involving the  $\pi$ -electrons of the aromatic/heterocyclic ring and vacant d-orbitals of the surface iron [16-17].

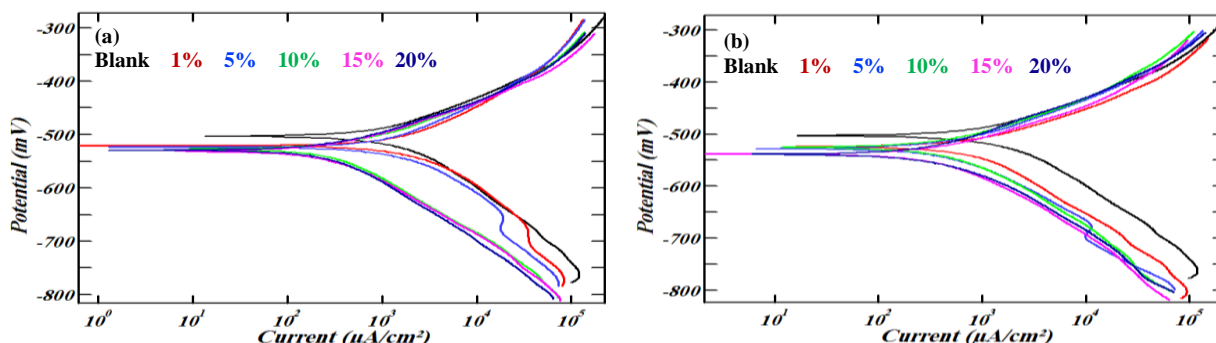


**Figure 6.** Polarization curves for carbon Steel in 1 M HCl with and without 1, 5, 10, 15% and 20% of (a) PF-T and (b) PL-T extracts at 60°C.

**Table 4.** Electrochemical parameters for Carbon Steel in 1 M HCl with and without 1, 5, 10, 15% and 20% of PF-T and PL-T extracts at 60°C.

Inhibitor Extract	Concentration (v/v)%	-E <sub>corr</sub> (mV)	$\beta_a$ (mV)	$\beta_c$ (mV)	I <sub>corr</sub> (mA cm <sup>-2</sup> )	C.R (mm/year)	E <sub>inh</sub> %
	Blank	-502	99	143	9.96	114.62	0
PF-T	1	-521	120	134	8.21	94.49	18
	5	-524	119	135	6.96	73.65	36
	10	-525	94	115	3.31	38.11	67
	15	-532	83	116	2.81	32.42	72
	20	-529	86	119	2.15	24.75	78
PL-T	1	-522	98	138	5.99	68.84	40
	5	-522	99	139	3.72	42.82	63
	10	-527	100	142	2.82	32.43	72
	15	-539	98	138	2.33	26.81	77
	20	-540	87	133	1.93	22.15	81

### 3.3. Adsorption isotherm and thermodynamic parameters

To study the mechanism of adsorption of the treated inhibitors on the carbon steel surface, the Langmuir adsorption isotherm

were used. The Langmuir adsorption isotherm can be expressed by Eq. 2 [14-15]:

$$\frac{C_{inh}}{\theta} = \frac{1}{K_{ads}} + C_{inh} \tag{2}$$

where  $C_{inh}$  is the inhibitor concentration,  $K_{ads}$  is the adsorption equilibrium constant, and  $\theta$  is the surface coverage and calculated by the ratio  $(E_{inh}\%)/100$  (Tables 2 and 3). Figure. 7 illustrates the Langmuir isotherms at different temperatures.

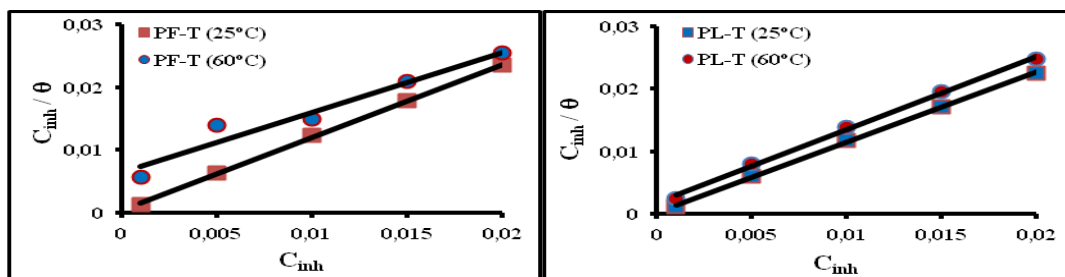


**Figure 7.** Langmuir isotherm for the adsorption of PF-T and PL-T extracts on the surface of the carbon steel.

The  $K_{ads}$  and  $R^2$  values are listed in Table 5, where  $R^2$  is correlation coefficient, which is the degree of fit between the experimental data and the isotherm equation. The plot showed good linearity, with  $R^2$  values very close to unity, indicating that the Langmuir model is suitable for describing the adsorption process. It additionally indicates strong adsorption of **PF-T** and **PL-T** on carbon steel's surface [18].

The inhibitor molecules gained stability when their free energies were reduced by their adsorption on the carbon steel surface, where they rearrange themselves or react with the ions or molecules near the surface [10]. The adsorption free energy  $\Delta G^{\circ}_{ads}$  was determined using Eq. 5:

$$\Delta G^{\circ}_{ads} = -RT \ln(55.5 K_{ads}) \tag{5}$$

where  $R$  is the universal gas constant,  $T$  is the absolute temperature, and the molar heat of adsorption of water is 55.5.

The  $\Delta G^{\circ}_{ads}$  value gives information about the spontaneity and type of adsorption. If  $\Delta G^{\circ}_{ads}$  is between  $-20$  and  $-40$  kJ/mol, the adsorption could proceed via physisorption and chemisorption (mixed adsorption) and if it more than  $-40$  kJ/mol, the adsorption type would be chemisorption. Chemisorption occurs via sharing or transfer of charge from the inhibitor molecule to the carbon steel surface to form a covalent bond, while physisorption involves electrostatic attraction between the charged carbon steel surface and the charged inhibitor molecules [19]. The  $\Delta G^{\circ}_{ads}$  values for all inhibitors at different temperature reach  $-20$  kJ/mol. The negative value of  $\Delta G^{\circ}_{ads}$  means that the adsorption is spontaneous and the value itself means that the adsorption type is mixed.

**Table 5.** Langmuir adsorption isotherm parameters for adsorption of PF-T and PL-T extracts on the surface of the carbon steel.

Inhibitor	PF-T		PL-T	
	25°C	60°C	25°C	60°C
Slope	1.17	0.96	1.12	1.17
Intercept	0.0004	0.006	0.0003	0.002
$R^2$	0.999	0.949	1	0.998
$K_{ads}$	2500	156	3333	556
$\Delta G^{\circ}_{ads}$ (KJ/mol)	-29.34	-25.10	-30.05	-28.62

Activation parameters  $E_a^*$ ,  $\Delta H_a^*$ ,  $\Delta S_a^*$

The activation energy can be calculated from Eq. 6:

$$\ln \left[ \frac{I_{corr2}}{I_{corr1}} \right] = \frac{E_a^*}{R} \left[ \frac{1}{T_1} - \frac{1}{T_2} \right] \quad (6)$$

$\Delta H_a^*$  can also be calculated from Eq. 7:

$$\ln \left[ \frac{I_{corr2} * T_1}{I_{corr1} * T_2} \right] = \frac{\Delta H_a^*}{R} \left[ \frac{1}{T_1} - \frac{1}{T_2} \right] \quad (7)$$

where  $E_a^*$  is the apparent activation energy,  $\Delta H_a^*$  is the activation enthalpy, R is the molar gas constant,  $I_{corr1}$  and  $I_{corr2}$  are the corrosion rates at the absolute temperatures  $T_1$  and  $T_2$ , respectively. The calculated activation energies  $E_a^*$  and  $\Delta H_a^*$  are listed in Table 4.

The  $E_a^*$  and  $\Delta H_a^*$  values were calculated for carbon steel corrosion both in the absence and the presence of 20% **PF-T** and **PL-T**. The table shows that the  $E_a^*$  values are increased in the presence of the inhibitor, indicating that the adsorption type is physisorption. They are also less than the value required for chemisorption (80 kJ/mol). This means that physisorption or chemisorption between the inhibitor and the carbon steel surface are weak [20-21]. Szauer explained that the  $E_a^*$  values increase due to the low adsorption strength of the inhibitor on the carbon steel surface with increasing temperature. A corresponding increase in the corrosion rate occurs because of the greater area of metal that is consequently exposed to the acidic environment [21].

The activation enthalpy values are positive both in the absence and presence of inhibitor, reflecting the endothermic nature of carbon steel corrosion. The  $\Delta H_a^*$  values for carbon steel in 20% **PF-T** and **PL-T** are higher than that solution without the corrosion inhibitor, indicating efficient protection against corrosion [22].

The average difference between  $E_a^*$  and  $\Delta H_a^*$  ( $E_a^* - \Delta H_a^*$ ) is 2.62 kJ/mol, which is approximately equal to the average value of  $RT$  (2.77 kJ/mol) at 333 K of the domain studied, indicating that the corrosion process is analogous to gas reaction, the evolution of hydrogen gas being associated with a decrease in the total corrosion rate. Moreover, this result is consistent with the fact that corrosion involves a unimolecular reaction [20], as reflected by the ideal gas known relationship:

$$E_a^* - \Delta H_a^* = TR \quad (8)$$

The entropies of activation ( $\Delta S_a^*$ ) for the corrosion of carbon steel in 1 M HCl solution in the absence and presence of **PF-T** and **PL-T** were calculated using the Arrhenius equation:

$$\ln \left[ \frac{I_{cor}}{T} \right] = \ln \left[ \frac{R}{Nh} \right] + \left[ \frac{\Delta S_{ads}^{\circ}}{R} \right] - \left[ \frac{\Delta H_{ads}^{\circ}}{R} \right] \quad (9)$$

where h is the Plank's constant ( $6.626176 \times 10^{-34}$  J.s) and N is the Avogadro's number ( $6.02252 \times 10^{23}$  mol<sup>-1</sup>). The  $\Delta S_a^*$  values of are listed in Table 6, and the values are negative for both the cases. A negative  $\Delta S_a^*$  value indicates that the corrosion process is controlled by the activation complex [19,23].

A closer look at the  $\Delta S_a^*$  values shows that the values shift in the positive direction in the presence of the extracts due to the formation of the adsorbed layer on the metal surface, which should increase disorder of the system. The inhibitor layer impedes the liberation of hydrogen ions at the metal surface, causing increased disorderliness and raising the entropy of the system [24-25].

The many compounds present in the extract make the active inhibitive components. Consequently, the focus of this effort has been to develop and treatment an inexpensive natural extraction product by natural product, which that effectively inhibits corrosion.

**Table 6.** Thermodynamic activation parameters of carbon steel in 1 M HCl at absence and presence of PF-T and PL-T extracts.

Medium	$E^{\circ}_{ads}$ (kJ/mol)	$\Delta H^{\circ}_{ads}$ (kJ/mol)	$\Delta S^{\circ}_{ads}$ (J/mol.K)
1 M HCl	19	16	-179
PF-T	27	25	-166
PL-T	31	29	-154

#### 4. CONCLUSION

- The potentiodynamic polarization measurement demonstrated that the treated and untreated **PF** and **PL** extracts act as effective inhibitors of carbon steel corrosion in 1 M HCl.
- Inhibition efficiency increases with increasing concentration of the palm extracts.
- The adsorption of the palm extracts on the carbon steel surface in 1 M HCl follows the Langmuir adsorption isotherm.
- The calculated  $\Delta G^{\circ}_{ads}$  values revealed that the adsorption process is spontaneous, and the inhibitor molecules are adsorbed on the metal surface through mixed adsorption (both physisorption and chemisorption).
- The values of the activation parameters  $E^*_a$ ,  $\Delta H^*_a$ , and  $\Delta S^*_a$  increased in the presence of the inhibitor, implying that physical adsorption or chemical bonding between the inhibitor and the carbon steel surface are weak. This also means that the corrosion process is endothermic, and is controlled by the activation complex.

#### References

1. G. M. Al-Senani, *Int. J. Electrochem. Sci.*, 11 (2016) 291.
2. G. M. Al-Senani, *World Appl. Sci. J.*, 33 (2015) 1659.
3. G. M. AL-Senani, S. I. AL-Saeedi, R. S. AL-Mufarij, *J. Mater. Environ. Sci.*, 7 (2016) 2240.
4. M. Sangeetha, S. Rajendran, J. Sathiyabama and P. Prabhakar, *J. Nat. Prod. Plant Resour.*, 2 (2012) 601.
5. L. A. Nnanna, I. O. Owate, O. C. Nwadiuko, N. D. Ekekwe, W. J. Oji, *Int. J. Mater. Chem.*, 3 (2013) 10.
6. W. Yang, Q. Wang, K. Xu, Y. Yin, H. Bao, X. Li, L. Niu and S. Chen, *Materials*, 10 (2017) 956.
7. H. H. Al-Sahlane, A. A. Sultan, M. M. Al-Faize, *Aquat. Sci. Technol.*, 1(2013) 135.
8. Salman Zafar, EcoMENA "Echoing Sustainability in MENA", <https://www.ecomena.org/>, (2017).
9. <http://www.rgbstock.com/photo/mixXIDy/Palm+leaves>.
10. A. S. Fouda, G. Y. Elewady, K. Shalabi and S. Habouba, *Int. J. Adv. Res.*, 2 (2014) 817.

11. N. Lahhit, A. Bouyanzer, J. Desjobert, B. Hammouti, R. Salghi, J. Costa, C. Jama, F. Bentiss and L. Majidi, *Port. Electrochem. Acta*, 29 (2011) 127.
12. L. A. Nnanna, K. O. Uchendu, F.O. Nwosu, U. Ihekoronye, E. P. Eti, *Int. J. Mater. Chem.*, 4 (2014) 34.
13. A. Hamdy, N. Sh. El-Gendy, *Egypt. J. Pet.*, 22 (2013) 17.
14. S. Aribo, S. J. Olusegun, L. J. Ibhadiyi, A. Oyetunji, D. O. Folorunso, *J. Assoc. Arab Univ. Basic Appl. Sci.*, 24 (2017) 34.
15. H. S. Gadaw and M. M. Motawea, *RSC Adv.*, 7 (2017) 24576.
16. M. Yadav, L. Gope, N. Kumari, P. Yadav, *Journal of Molecular Liquids*, 216 (2016) 78.
17. A. Singha, V. K. Singh, M. A. Quraishi, *J. Mater. Environ. Sci.*, 1 (3) (2010) 162.
18. G. M. AL-Senani<sup>1,2</sup>, S. I. AL-Saedi<sup>1,2</sup>, R. S. AL-Mufarij, *Orient. J. Chem.*, 31(2015) 2077.
19. S. Kr. Saha, A. Dutta, P. Ghosh, D. Sukul and P. Banerjee, *Phys. Chem. Chem. Phys.*, 17 (2015) 5679.
20. M. Majeed, A. Sultan and H. Al-Sahlane, *J. Chem. Pharm. Res.*, 6 (2014) 996.
21. S. Andreani, M. Znini, J. Paolini, L. Majidi, B. Hammouti, J. Costa, A. Muselli, *J. Mater. Environ. Sci.* 7 (2016) 187.
22. S. Merah, L. Larabi, O. Abderrahim, Y. Harek, *Int J Ind Chem*, 8 (2017) 263.
23. M. Dahmani, A. El-Touhami, S.S. Al-Deyab, B. Hammouti, A. Bouyanzer, *Int. J. Electrochem. Sci.* 5 (2010) 1060.
24. H. Zarrok, R. A. Salghi, M. Assouag, B. Hammouti, H. Oudda, S. Boukhris, S. S. Al Deyab, I. Warad, *Der Pharmacia Lettre*, 5 (2013) 43.
25. E. F. Olasehinde, S. J. Olusegun, A. S. Adesina, S. A. Omogbehin, Momoh-Yahayah, *H. Nat. Sci.* 11 (2013) 83.

© 2018 The Authors. Published by ESG ([www.electrochemsci.org](http://www.electrochemsci.org)). This article is an open access article distributed under the terms and conditions of the Creative Commons Attribution license (<http://creativecommons.org/licenses/by/4.0/>).